ELSEVIER

Biophysical Chemistry 99 (2002) 31–41

Biophysical Chemistry

www.elsevier.com/locate/bpc

Antibody/antigen affinity behavior in liquid environment with electrical impedance analysis of quartz crystal microbalances

J. Zhang*, X.D. Su, S.J. O'Shea

Institute of Materials Research and Engineering, 3 Research Link, Singapore 117602, Singapore

Received 13 January 2002; received in revised form 9 April 2002; accepted 11 April 2002

Abstract

Electrical impedance analysis has been used to study anti-human immunoglobulin G (anti-h IgG) adsorption and the subsequent human immunoglobulin G (hIgG) or rabbit immunoglobulin G (rIgG) affinity reaction in aqueous liquids on a polystyrene (PS)-modified quartz crystal microbalance (QCM) surface. Time-dependent adsorption data of both the frequency shift and the electrical equivalent parameters (motional resistance, shunt capacitance, quality factor, etc) are monitored. It was found that the motional resistance, R, increases while the resonance frequency, f, decreases during both the anti-h IgG immobilization and the subsequent affinity process. Decreasing f primarily arises from the increased mass loading. Increasing R indicates more power dissipation (increased losses) in the system. The change in motional resistance, ΔR, in the affinity reaction is considerably larger than that in anti-h IgG immobilization adsorption process, although the resonant frequency shifts, Δf, are very close in these two processes. Specifically, for a saturated solution, the ratio of $\Delta R/\Delta f$ is 9.45×10^{-3} Ω/Hz for anti-h IgG adsorption and 28.1×10^{-3} Ω/Hz for anti-h IgG/hIgG binding respectively, indicating the increased power dissipation with the increasing binding molecules. The shunt capacitance changes little in the hIgG binding process ($\sim$0.01 pF). © 2002 Elsevier Science B.V. All rights reserved.

Keywords: Impedance analysis; Equivalent circuit; Quartz crystal microbalances; Antigen/antibody affinity; Resonant frequency

1. Introduction

The quartz crystal microbalance (QCM) is an ultra-sensitive weighing device. For a quartz crystal oscillating in the thickness shear mode, the shift in resonance frequency is linearly related to the loading mass by the well-known Sauerbrey equation [1]. By measuring the resonant frequency, mass loading below 1 ng/cm^2 can be determined [2,3]. Although originally used as mass detectors for solid thin films, an important new application was demonstrated by Nomura et al. [4] showing that the QCM can be operated in liquid, preferably in an arrangement where only one face of the crystal is exposed to the liquid and the other to the gas phase. This has led to the development of electrochemical quartz crystal microbalance (EQCM) for electrochemical application [5], and applications of QCM as a biosensor in the liquid

*Corresponding author. Tel.: +65-874-8109; fax: +65-872-7528.

E-mail address: j-zhang@imre.org.sg (J. Zhang).

PII: S0301-4622(02)00109-6

phase to study processes such as protein adsorption [6,7], antibody/antigen binding [3,8,9], and the adhesion of large biological molecules such as cells [10,11].

The Sauerbrey equation is valid for acoustically thin, evenly distributed, rigid and non-porous overlayers added to or removed from the QCM electrode. In chemical sensing applications, however, many coating materials do not act as thin uniform rigid layers. Many films show viscoelastic behavior, which can cause significant differences in the sensor response compared to a corresponding rigid layer. This is particularly the case in liquid environments, where the viscous properties of the surrounding liquid or solvent molecules that penetrate the adsorbed films can strongly influence the QCM responses. Thus, the coating thickness or adsorbed mass calculated from the observed frequency shift using the Sauerbrey equation may differ from the real value, if the influence of the viscoelasticity has not been taken into account [12–15].

In the case of the adsorption of a non-rigid overlayer it is clear that measurement of the frequency shift alone cannot supply sufficient information. As in any general resonating system, in addition to the resonance frequency, f, the damping behavior of the crystal is also required [15–28]. There are two main methods used to evaluate QCM damping behavior. One was developed by Rodahl et al. [15–21] to measure the dissipation factor D (inversely proportional to the quality factor (Q-factor)) from a non-driven (i.e. freely oscillating) crystal. The other technique is to monitor the variations of motional resistance by electrical impedance analysis [22–28] since the motional resistance acts as an indicator of viscoelastic loss [25].

In this work, we simultaneously measured the resonance frequency and the motional resistance of a polystyrene (PS)-modified QCM operating in aqueous solutions. A Network Analyzer was used to record the QCM response to anti-human immunoglobulin G (anti-h IgG) adsorption and the subsequent affinity reaction of the surface with either human immunoglobulin G (hIgG) or rabbit immunoglobulin G (rIgG). The motional resistance change resulting from different processes was measured and related to the resonator damping. The relationship between the resonance frequency shift and the motional resistance change during affinity reaction were also investigated.

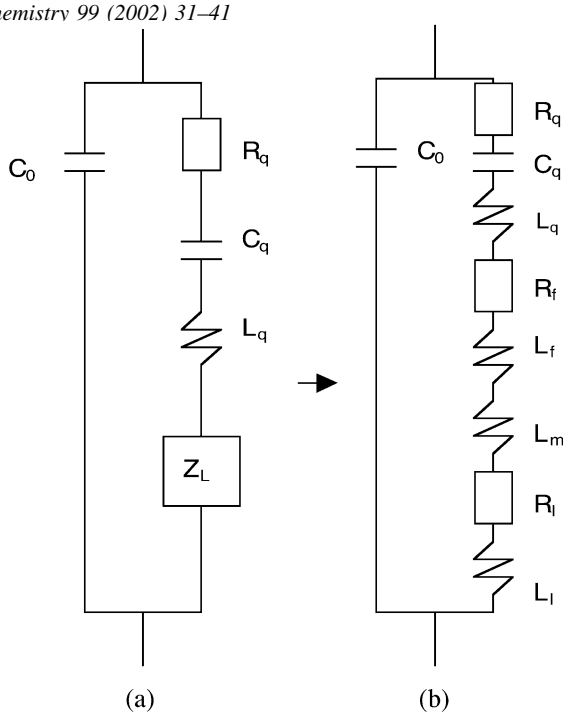

Fig. 1. (a) Electrical equivalent circuit model of a QCM with an arbitrary surface load (Z_l); and (b) Lumped-element electrical equivalent circuit model for a QCM coated with a viscoelastic layer in contact with a semi-infinite Newtonian liquid.

2. Theory

Typically, a quartz crystal can be simulated by the Butterworth–van Dyke electrical equivalent circuit [29,30], which consists of a motional branch in parallel with a shunt capacitance C_0 (due to the connections, cables and the quartz itself) as shown in Fig. 1a. The motional branch consists of a series RLC circuit where R_q represents the damping friction, L_q the inertia and C_q the quartz compliance of the bare quartz resonator.

The impedance Z_L is the experimental quantity of interest and represents the changes caused by any surface load. The form of Z_L depends on the specific experimental conditions. In this work we follow Granstaff and Martin [29] and use the equivalent circuit for Z_L shown in Fig. 1b, which

represents a viscoelastic film (parameters L_m, L_f, R_f) in contact with a bulk Newtonian liquid (parameters R_l, L_l). This equivalent circuit model has proved appropriate for viscoelastic loads in many QCM applications [31,32] provided that, (a) Z_L is much smaller than the characteristic quartz impedance, $Z_q = \sqrt{\rho_q \mu_q}$, where ρ_q is the quartz density, and μ_q the quartz shear stiffness; and (b) the acoustic impedance match at the film/liquid interface reflects back most of the vibrational energy. Both of these conditions apply in this study, and hence for the circuit of Fig. 1b,

$$Z_L = R_q + R_f + R_l + j(L_q + L_f + L_l + L_m) \quad (1)$$

The physical interpretation of the circuit elements is that resistance (R) represent acoustic energy dissipation whereas the inductance (L) is the mass loading (L_m is the mass load of the film, L_f and L_l are the viscoelastic inertial mass for the film and liquid respectively). Experiments relating R and L to specific properties of the overlayer materials (e.g. density, shear modulus, etc) are given in the literature [31]. In this work we are primarily concerned with the measurement of changes in R_f using impedance analysis which occur during antigen/antibody reactions. Specifically, we calculate the total motional resistance change (ΔR) which occurs during adsorption, namely,

$$\Delta R = \Delta R_l + \Delta R_f \quad (2)$$

where ΔR_l and ΔR_f reflect changes in energy dissipation in the thin film coating or liquid medium, respectively. It is hoped that such data can yield useful and robust signals for use in antigen/antibody QCM sensors in addition to the measurement of adsorption induced frequency shifts. Note that, within the equivalent circuit models, the series resonance shift Δf is given by [31]:

$$\Delta f = -f_0\left(\frac{\Delta L}{2L_q}\right) \quad (3)$$

where f_0 is the fundamental resonance frequency and ΔL the measured change in inductance. It is found in this work and in previous studies [31] that the contribution to ΔL from the viscoelastic masses (L_f, L_l) is small for thin polymer films ($\sim < 1$ μm) and the principal contribution is the pure gravimetric mass loading (L_m). Hence, for the IgG affinity reaction studied in this work, we concentrate on understanding viscoelastic behavior through the dissipation term (R) rather than the much smaller effects evident in the inductance or capacitance.

3. Experimental

3.1. Reagents and apparatus

PS (MW 670 000), anti-h IgG, hIgG and rIgG was purchased from Sigma Aldrich (St. Louis, MO). Reaction buffer was 50 mM of phosphate buffered saline (PBS, pH 7.4) (PBS was prepared by mixing 8.0 mM Na_2HPO_4, 1.5 mM KH_2PO_4 (pH 7.2), 137 mM NaCl and 2.7 mM KCl). Other chemicals used were certified reagents of analytical grade from Fluka (Buchs, Switzerland) or Sigma. De-ionized Water (resistance of 18 MΩ·cm) was obtained from a Milli-Q unit (Millipore Inc.).

Unpolished AT-cut quartz crystals (10 MHz, 14 mm diameter) with 5.1 mm gold electrodes (International Crystal Manufacturing, Oklahoma City, OK) were used. The electrodes were composed of a 50A Cr underlayer and a 1000A Au top layer. The calculated mass sensitivity using the Sauerbrey equation is ~ 4.4 ng/Hz cm^2. The quartz crystal was mounted by concentric rubber seals (O-ring) into a cell to provide contact with one side of the quartz crystal to the liquid. The cell was made of Plexiglas and allowed an application of liquid volume ~ 1 ml. Measurements were performed on an anti-vibration platform (Newport, USA). All processes were undertaken at a temperature of 23 ± 0.3 °C.

A S&A 250B Network Analyzer (Saunders & Associates, Inc., USA, with Frequency range 1 MHz–100 MHz; Frequency correlation 2 ppm at series) was used and the quartz crystal was connected through a standard 250B network analyzer test head. An automatic gain control (AGC) maintains a voltage (or power) level proportional to the loss of the QCM while simultaneously tracking the resonant frequency. This allows for measure-

Table 1
Changes in electrical parameters of QCM arising from coating with PS, clamping into the liquid cell, and injection of the buffer injection[a]

Parameters	PS modification		Clamping	Buffer injection (50 μl)
	Uncoated	Coated		
Resonant frequency, f_0 (Hz)	10 008 230 ± 2	10 004 498 ± 1	10 004 644 ± 1	10 001 330 ± 2
Motional resistance, R (Ω)	7.4701 ± 0.0103	7.9549 ± 0.0153	11.7965 ± 0.0201	242.8307 ± 0.1084
Motional capacitance, C (fF)	28.4182 ± 0.1508	28.7985 ± 0.0187	28.7772 ± 0.0034	31.2894 ± 0.1086
Motional inductance, L (mH)	8.8872 ± 0.0455	8.7875 ± 0.0065	8.8054 ± 0.0019	8.0891 ± 0.0357
Quality factor, Q (k)	74.87 ± 0.42	69.42 ± 0.13	46.76 ± 0.08	2.09 ± 0.01
Shunt capacitance, C_0 (pF)	6.02 ± 0.01	6.03 ± 0.01	6.10 ± 0.01	7.89 ± 0.01

[a] All values listed here are the average ones from 20 times experimental data.

ment of highly-damped QCM with good accuracy (~1 Hz) and repeatability.

3.2. Procedures

3.2.1. Preparation and characterization of polymer films

PS coatings have been intensively used with QCMs for antigen/antibody affinity detection [32,33]. PS does not cause significant damping nor show high viscoelastic contribution to the frequency shift, even with thick coatings [34]. PS films are made by dip-drying, i.e. dipping the clean crystals into a PS solution (2–5 wt.% in toluene) for 30 min followed by removal and drying. To ensure a uniform spread of thin film, the crystals were lain horizontally. Before coating, the metal electrodes were carefully washed for 30 min in acetone followed by distilled water and dried with nitrogen. The adhesion of the PS film was improved by exposing the coated QCM to ambient air for 30 min or by heating at 100 °C for 15 min. The resulting PS films are typically ~100 nm thick.

3.2.2. In situ frequency and equivalent circuit parameters measurement of antigen/antibody in buffer

After the dip-drying process, the PS-modified crystal was clamped between two O-rings with one surface exposed to liquid, and 50 μl of PBS buffer solution was injected into the cell. Subsequently, after stable conditions had been reached, 5 μl anti-h IgG and hIgG or rIgG solution (of varying concentration) was injected successively. The resonant frequency and equivalent circuit parameters were recorded simultaneously for all of the above procedures. In all experiments, the PBS buffer volume is fixed at 50 μl and the anti-h IgG solution concentration is fixed at 2.5 mg/ml. The liquid cell holder and electrical connections were not adjusted throughout the experiment.

Prior to every experiment, the S&A analyzer and the test fixture were calibrated and compensated with the standard impedance kits. The S&A equivalent circuit measurement has a processing time of approximately 0.2–0.5 s per data cycle, thus allowing for real-time monitoring. In our measurement, the data collection time interval is 5 s/point.

4. Results and discussion

Prior to measurements of anti-h IgG adsorption and IgG affinity reaction, the electrical parameters of QCM sensors under different processes conditions were measured. The parameters are shown in Table 1 for the uncoated QCM sensor, the QCM coated with PS, the QCM clamped into the liquid cell (no liquid injection), and the effect of adding the buffer solution.

From this data, the relative changes in the parameters (ΔL, ΔR, ΔC) can be used to find each of the equivalent circuit elements for the PS films and the added liquid [31]. It is clear from Table 1 that although the PS coating and the liquid cell clamping perturb the QCM response, by far the largest variation occurs on injection of the buffer

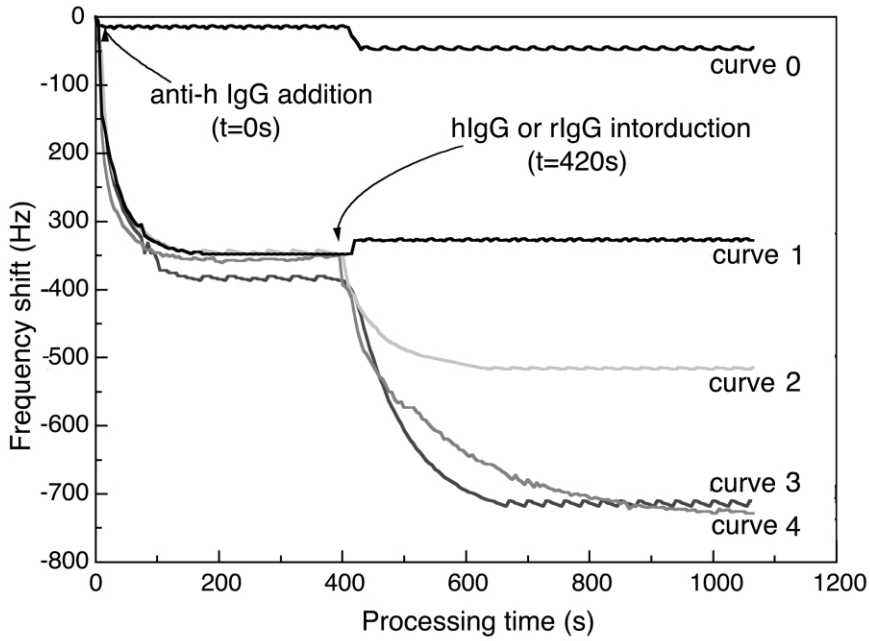

Fig. 2. Typical frequency shift of a PS coated 10 MHz QCM exposed to anti-h IgG application at $t=0$ and subsequently rIgG (curve 1), or hIgG (curve 2–4) at $t=420$ s. Curves 2, 3, 4 represent hIgG concentrations of 23.8, 95.2 and 238 μg/ml, respectively. Curve 0 is a control experiment showing the injection of 5 μl PBS buffer added at $t=0$ and $t=420$ s, respectively.

liquid. (The resonator frequency shifts by -3314 ± 200 Hz and the Q-factor decreases from ~47 000 to ~2000). Also note the stability of the measurements. Using the shift in resonance frequency between the uncoated and coated QCM we estimate that the PS overlayer is of thickness $h_f=78$ nm, as calculated using the Sauerbrey equation and assuming a PS density of 1.06×10^3 kg/m^3 [34].

4.1. IgG reaction–frequency shift

In the affinity experiments, anti-h IgG is first immobilized on the PS surface followed by the affinity reaction using hIgG or rIgG. Fig. 2 shows a typical response for the QCM frequency shift measured in situ for the reactions. Buffer pH and the concentration of coating protein are major factors influencing the immobilization step. In these experiments, 5 μl of anti-h IgG solution (2.5 mg/ml) is introduced into 50 μl of PBS buffer in the liquid cell to give a final anti-h IgG concentration of 0.238 mg/ml. As shown in Fig. 2, the adsorption of anti-h IgG causes an initial rapid frequency decrease (~100 s) due to mass loading followed by a slower frequency decrease as the adsorption tends to saturate. The saturation frequency shift is -368 ± 20 Hz. We assume that the PS electrode is totally covered with anti-h IgG as our previous results indicate that saturation occurs above 0.2 mg/ml for this system [32]. In control experiments, 5 μl of PBS buffer with no anti-h IgG was added to the liquid cell and no significant frequency shift could be observed (curve 0 in Fig. 2).

Following anti-h IgG immobilization, rIgG (curve 1) and hIgG at different concentrations were introduced at time $t=420$ s. hIgG addition (curves 2–4) causes an initial rapid frequency decrease followed a slower decrease as the hIgG binding tends to saturate. A Langmuir type adsorption curve is observed. The affinity reaction of hIgG is essentially complete within 5–7 min. The frequency shift increases with increasing hIgG concentration, as shown in curve 2 (23.85 μg/ml) and curve 3 (95.25 μg/ml).

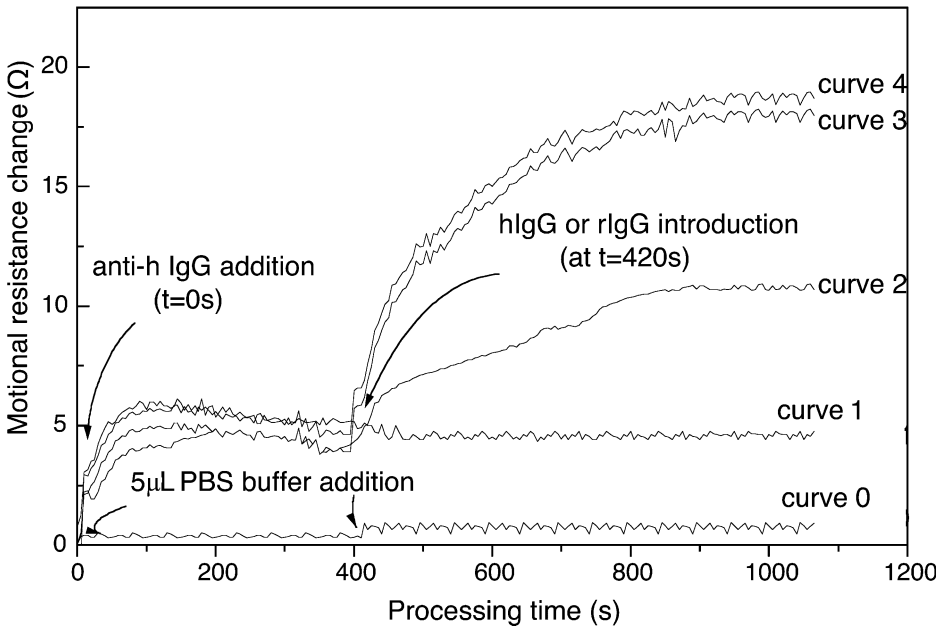

Fig. 3. Typical motional responses of a PS coated 10 MHz QCM to anti-h IgG application at $t=0$ and subsequently rIgG (curve 1), or hIgG (curve 2–4) at $t=420$ s. Curves 2, 3, 4 represent hIgG concentrations of 23.8, 95.2 and 238 μg/ml, respectively. Curve 0 is a control experiment showing the injection of 5 μl PBS buffer added at $t=0$ and $t=420$ s, respectively.

Curve 4 (238 μg/ml) is similar to curve 3 and indicates the onset of saturation, which occurs for hIgG concentrations greater than 100 μg/ml. The frequency shift for saturated hIgG adsorption is -365 ± 22 Hz, showing a 1:1 correspondence with the anti-h IgG adsorption sites (saturated frequency shift -368 ± 20 Hz). The mass loading at saturation is 1625 ng/cm^2 as calculated using the Sauerbrey equation.

Two control experiments are also shown in Fig. 2. Additions of PBS buffer (curve 0) and rIgG (curve 1) show only a small frequency jump on liquid injection and no indication of adsorption. The shunt capacitance changes are also negligible (<0.01 pF) during the protein adsorption experiments.

4.2. IgG reaction-motional resistance

Fig. 3 shows the in situ changes in motional resistance (ΔR) corresponding to the IgG/anti-h IgG experiments of Fig. 2. It is observed that the injection of anti-h IgG causes a rapid increase in motional resistance (within ~3 min) which thereafter decreases slightly with time. The final resistance change due to anti-h IgG immobilization is approximately 4–5 Ω, i.e. $\Delta R=4$–5 Ω. Different solutions were introduced as shown at time $t=420$ s. For hIgG adsorption (curve 2–4), the motional resistance increases in analogy with the frequency decrease and reaches a stable value within ~8 min. The motional resistance change increases with IgG concentration and saturates at high hIgG concentrations. The saturated resistance change is approximately 10–12 Ω, i.e. $\Delta R=10$–12 Ω. As in the frequency data of Fig. 2, there is little change in ΔR (0.3 Ω) for the injection of PBS buffer (curve 0) and rIgG (curve 1). The negative results of such control experiments show that changes in motional resistance can be essentially associated with the changes in viscoelastic response of the PS films during hIgG adsorption, i.e. in the model of Fig. 1b, $\Delta R\approx\Delta R_f$. There are possibly some smaller changes resulting from the fluid resistance, ΔR_l, as noted below.

Thus, changes in the resistance can be used as

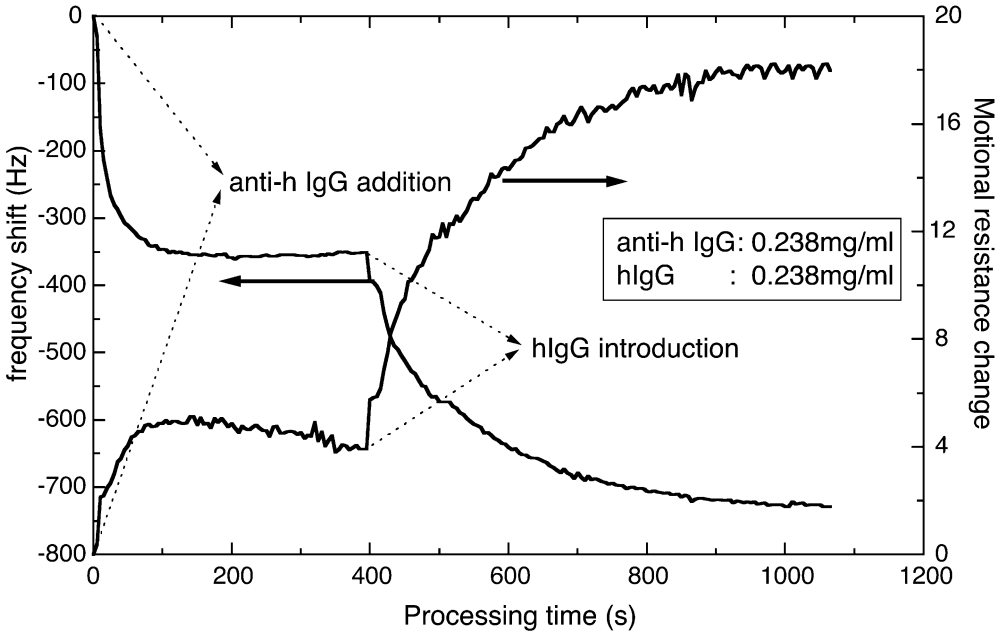

Fig. 4. Typical data showing the simultaneous measurement of the motional resistance change and the resonant frequency shift. Anti-h IgG (2.5 mg/ml, 5 μl) was successively introduced into 50 μl PBS buffer.

an additional parameter to monitor the anti-h IgG/IgG affinity reaction. Fig. 4 shows this clearly, demonstrating the correlation between the frequency shift and the corresponding motional resistance change for a fixed concentration anti-h IgG/IgG affinity test. The frequency shift depends on both the gravimetric (L_m) and the viscoelastic inertial (L_f) contributions to the mass loading and to separate these effects requires a measurement of the complex shear modulus of the films. For QCM systems very similar to those used in this study, it is found that gravimetric loading accounts for most of the frequency shift on adsorption [31]. There is minimal effect on the frequency shift arising from the change in R. This can be verified by finding the Q-factor of the resonator, as shown in Fig. 5. The data shows that for the anti-h IgG/IgG processes outlined above, the Q-factor decreases from $\sim$2050 to $\sim$1950. Such a small change in Q for a weakly-damped system shifts the resonance frequency by a negligible amount ($\ll$1 ppm). For completeness, we note that the addition of anti-h IgG or hIgG does not significantly change the shunt capacitance, C_0, ($<$0.001 pF). Shunt capacitance changes are mainly contributed by ion concentration changes in the solution. Thus, to a good approximation for the anti-h IgG/IgG system, the frequency signal represents pure mass loading and the extra signal afforded by the resistance change gives the adsorption induced energy dissipation, just as shown in Fig. 6.

The motional resistance change and associated energy dissipation mechanism of a QCM operating in aqueous solutions has been investigated previously [14–28]. The observed increase in motional resistance (i.e. dissipation) on protein adsorption and affinity reaction can, in principle, originates from three mechanisms, namely: (i) macroscopic interactions at the protein/substrate interface (viscous slip, surface roughness, etc); (ii) macroscopic interactions at the protein/liquid interface (liquid density, viscosity, protein concentration, etc) and (iii) microscopic processes within the protein layer (effect of entrapped liquid, porosity, etc) [15].

We assure that (i) can be ignored in our case. Previous research has shown that only proteins bonded firmly on a PS-modified QCM surface can be sensed and hence little or no slip occurs at the

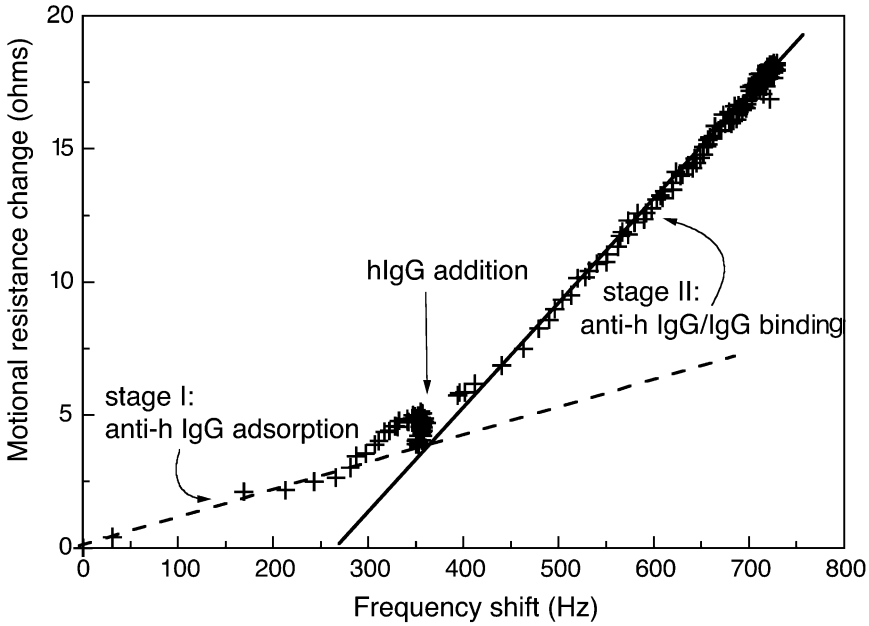

Fig. 5. Typical data showing the relationship ($\Delta R/\Delta f$) between the motional resistance and the resonant frequency shift. (a) Anti-h IgG (2.5 mg/ml, 5μl) was successively introduced into 50 μl PBS buffer.

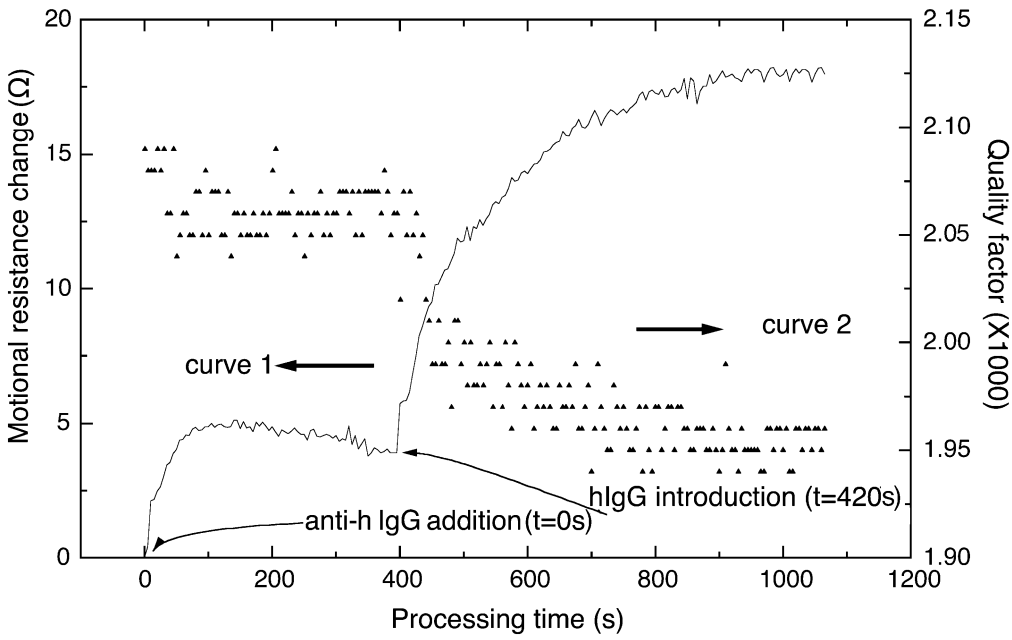

Fig. 6. Measured changes of *Q*-factor with the processing time. Both anti-h IgG adsorption and hIgG binding processes will result in a decreasing *Q*-factor.

QCM/anti-h IgG interface or the hIgG/liquid interface [10,15,17,19]. It has also been shown that the resistance change due to the surface roughness is small compared to the total sensor response [15].

Changes in liquid properties (ii) may contribute to changes in ΔR. Figs. 4 and 5 show that on injection of anti-h IgG or IgG solutions there is a sharp initial change in motional resistance. The magnitude of the jump in resistance is always less than 3 Ω, i.e. $\Delta R_l = 3\ \Omega$.

The change in motional resistance caused by the liquid can be analyzed using Matin's equations [29]:

$$R_l = \frac{\pi}{4K^2 C_0 Z_q}\sqrt{\frac{\rho_l \eta_l}{2\omega_s}} \quad (4)$$

where Z_q ($=8.84\times10^6$ N/m^2 s), ω_s and C_0 are the characteristic impedance, angular resonant frequency and shunt capacitance ($C_0 = 6.02$ pF for our QCM) of the quartz crystal in air, respectively. ρ_l, is the density and η_l the viscosity of liquid. K^2 ($=7.74\times10^{-3}$) is the electromechanical coupling factor for quartz [30]. The calculated value is $R_l = 240.5\ \Omega$ assuming a buffer solution of $\rho_l = 1\times10^3$ kg/m^3 and $\eta_l = 1\times10^{-3}$ mPa/s [28], which corresponds well with the measured result in Table 1 (226.1 Ω). The injected protein solutions will change the density and viscosity of the liquid. If we assume a $\pm1\%$ variation in the product $\rho_l\eta_l$, which is not unreasonable, then the calculated variation in R_l is $\Delta R_l \sim 2$–$3\ \Omega$, which is of the same order as the measured data. As noted previously (see curve 0, Fig. 4), the change in ΔR_l due to the additional volume of injected pure PBS buffer is always negligible or very small ($<0.6\ \Omega$).

From the above discussion we therefore find that the maximum variation of ΔR_l is $\sim3\ \Omega$. For the anti-h IgG adsorption process on PS, the change in motional resistance is only ~4–$5\ \Omega$. Thus, we cannot rule out that a significant fraction of the resistance change is due to the variation of the bulk liquid properties, i.e. $\Delta R = \Delta R_l + \Delta R_f$. For the anti-h IgG/IgG affinity reaction the total resistance change is much larger ($\Delta R = 10$–$12\ \Omega$) and in this case the adsorbed hIgG molecules play the key role in increasing the energy dissipation, i.e. case (iii) holds and $\Delta R \approx \Delta R_f$. The microscopic cause of the enhancement of the viscoelastic dis-

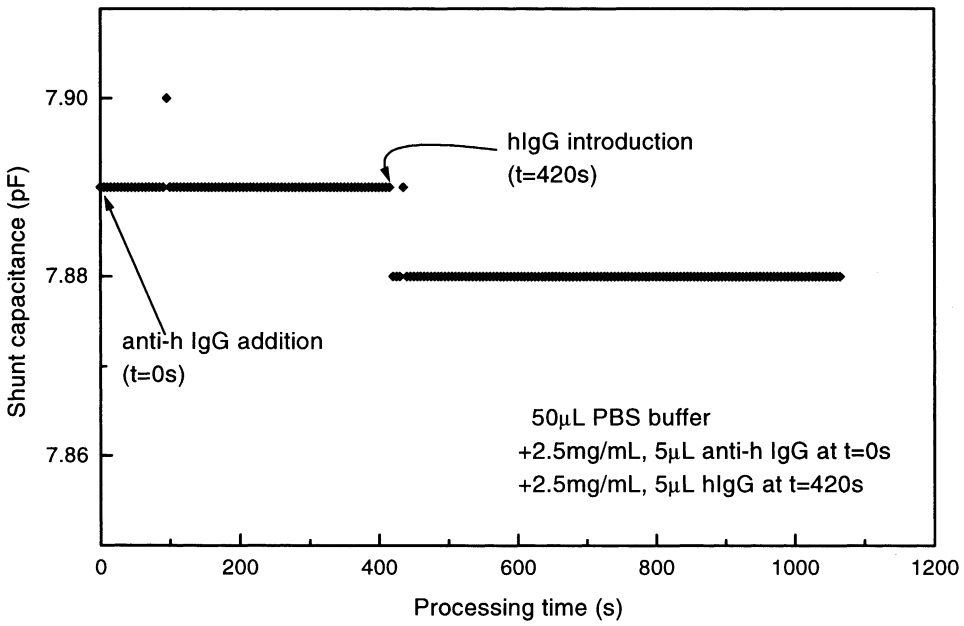

Fig. 7. Measured shunt capacitance change vs the processing time.

sipation is not known, but may arise from entrapment of viscous matter (e.g. water) within the protein layers, confirmational changes in the PS network by adsorption induced surface stresses, increasing biological film thickness, etc.

4.3. Ratio between ΔR and Δf

The ratio between the motional resistance change and the frequency shift ($\Delta R/\Delta f$) can be used as a criteria to evaluate the relative influence of viscoelastic and mass loading effects [13,22,26]. A high $\Delta R/\Delta f$ ratio implies an increased viscoelastic or damping contribution. Fig. 6 shows a plot of ΔR against Δf for the IgG affinity test. Note that the changes of slope in stage I (anti-h IgG adsorption) and stage II (anti-h IgG/IgG binding).

The $\Delta R/\Delta f$ ratio determined from the slope of the straight lines in the figure is 9.45×10^{-3} Ω/Hz in the anti-h IgG adsorption (stage I) and is 28.1×10^{-3} Ω/Hz in the hIgG binding process (stage II), respectively. The $\Delta R/\Delta f$ ratio in binding hIgG is much larger (~3 times) than that in the anti-h IgG adsorption onto the substrate, indicating that increased dissipation for a given mass adsorption.

Shunt capacitance changes in the whole process were also monitored and the results were shown in Fig. 7. It can be seen that the adsorption will cause the decreased capacitance values, which is probably due to the series capacitor formed by the adsorption antigen/antibody molecules.

5. Conclusions

The variations in the equivalent circuit parameters of a QCM can be monitored easily in real time using commercially available quartz crystal test equipment, e.g. S&A 250B Network Analyzer. We have demonstrated the ability of measuring the full equivalent circuit by monitoring the processes of anti-h IgG/IgG adsorption onto PS coated QCM. In particular it was shown that the motional resistance change, which is associated with energy dissipated during adsorption, can provide an useful measurement signal in addition to the frequency shift. For the IgG/anti-h IgG affinity reaction, the resistance change (10–12 Ω) was focused to be much larger than any changes arising from bulk liquid effects (~3 Ω), and must therefore be a reflection of microscopic processes arising from the IgG adsorption.

Acknowledgments

This research was sponsored by Agency of Sciences, Technology, and Research (A-Star) Grant 93/11/4-2, Singapore.

References

[1] G. Sauerbrey, The use of quartz oscillators for weighing thin layers and for microweighing, Z. Physik 155 (1959) 206–222.
[2] M. Thompson, G.K. Dhaliwal, C.L. Arthur, Liquid-phase piezoelectric and acoustic transmission studies of interfacial immunochemistry, Anal. Chem. 58 (1986) 1206–1209.
[3] M. Muratsugu, F. Ohta, Y. Miya, S. Kurosawa, N. Kamo, H. Ikeda, Quartz crystal microbalance for the detection of microgram quantities of human serum albumin: relationship between the frequency change and the mass of protein adsorbed, Anal. Chem. 65 (1993) 2933–2937.
[4] T. Nomura, M. Okuhara, Determination of lead by adsorption of the extracted 8-quinolinolate on the electrodes of a piezoelectric quartz crystals, Anal. Chim. Acta 143 (1982) 243–247.
[5] K.K. Kanazawa, O.R. Melroy, The quartz resonator: electrochemical applications, IBM J. Res. Dev. 37 (1993) 157–171.
[6] M. Laatikainen, M. Lindstro, Measurement of sorption in polymer membranes with a quartz crystal microbalance, J. Membr. Sci. 29 (1986) 127–141.
[7] J.J. Ramsden, J.J. Ramsden, Sensitivity enhancement of integrated optic sensors using Langmuir–Blodgett lipid films, Sens. Actuators B 16 (1993) 439–442.
[8] A. Janshoff, C. Steinem, M. Sieber, H. Galla, Specific binding of peanut agglutinin to GM1-doped solid supported lipid bilayers investigated by shear wave resonator measurements, Eur. Biophys. J. 25 (1996) 105–113.
[9] M.D. Ward, D.A. Buttry, In situ interfacial mass detection with piezoelectric transducers, Science 249 (1990) 1000–1007.
[10] D.M. Gryte, M.D. Ward, W.-S. Hu, Real-time measurement of anchorage-dependent cell adhesion using a quartz crystal microbalance, Biotechnol. Prog. 9 (1993) 105–108.

[11] C.E. Reed, K.K. Kanazawa, J.H. Kaufman, Physical description of a viscoelastically loaded AT-cut quartz resonator, J. Appl. Phys. 68 (1990) 1993–2001.
[12] D. Johannsmann, K. Mathauer, G. Wegner, W. Knoll, Viscoelastic properties of thin films probed with a quartz crystal resonator, Phys. Rev. B 46 (1992) 7808–7815.
[13] A. Janshoff, J. Wegener, M. Sieber, H.J. Galla, Double-mode impedance analysis of epithelial cell monolayers cultured on shear wave resonators, Eur. Biophys. J. 25 (1996) 93–103.
[14] M. Rodahl, F. Hook, A. Krozer, P. Brzezinski, B. Kasemo, A simple setup to simultaneously measure the resonant frequency and the absolute dissipation factor of a quartz crystal microbalance, Rev. Sci. Instrum. 67 (1996) 3238–3241.
[15] M. Rodahl, F. Hook, C. Fredriksson, A. Krozer, C.A. Keller, P. Brzezinski, M. Voinova, B. Kasemo, Simultaneous frequency and dissipation factor QCM measurements of biomolecular adsorption and cell adhesion, Faraday Discuss. 107 (1997) 229–246.
[16] F. Hook, M. Rodahl, C.A. Keller, K. Glasmastar, C. Fredriksson, P. Dahlqvist, B. Kasemo. The dissipative QCM-D technique: interfacial phenomena and sensor applications for proteins, biomembranes, living cells and polymers, Proceedings of IEEE International Frequency Control Symposium, (1999) 966–972.
[17] C. Fredriksson, S. Khilman, B. Kasemo, D.M. Steel, In vitro real-time characterization of cell attachment and spreading, J. Mater. Sci.: Mater. Med. 9 (1998) 785–788.
[18] F. Hook, M. Rodahl, P. Brzezinski, B. Kasemo, Structural changes in hemoglobin during adsorption to solid surfaces: effects of pH, ionic strength, and ligand binding, Proc. Natl. Acad. Sci. 95 (1998) 12271–12276.
[19] G. Nimeri, C. Fredriksson, H. Elwing, L. Liu, M. Rodahl, B. Kasemo, Neutrophil interaction with protein-coated surfaces studied by an extended quartz crystal microbalance technique, Colloids Surf. B 11 (1998) 255–264.
[20] F. Hook, M. Rodahl, P. Brzezinski, B. Kasemo, Energy dissipation kinetics for protein and antibody–antigen adsorption under shear oscillation on a quartz crystal microbalance, Langmuir 14 (1998) 729–734.
[21] C. Fredriksson, S. Khilman, M. Rodahl, B. Kasemo, The piezoelectric quartz crystal mass and dissipation sensor: a means of studying cell adhesion, Langmuir 14 (1998) 248–251.
[22] J. Zhang, W. Wei, A. Zhou, D. He, S. Yao, Q. Xie, A novel investigation of magnetic field effects on the sedimentation of erythrocytes with the series piezoelectric quartz crystal sensor, Colloids Surf. A 180 (2001) 155–161.
[23] Q. Xie, Y. Zhang, C. Xiang, J. Tang, Y. Li, Q. Zhao, S. Yao, A comparative study on the viscoelasticity and morphology of polyaniline films galvanostatically grown on bare and 4-aminothiophenol-modified gold electrodes using an electrochemical quartz crystal impedance system and SEM, Anal. Sci. 17 (2001) 613–620.
[24] A. Zhou, Q. Xie, P. Li, L. Nie, S. Yao, Piezoelectric crystal impedance analysis for investigating the modification processes of protein, cross-linker, and DNA on gold surface, Appl. Surf. Sci. 158 (2000) 141–146.
[25] R. Lucklum, C. Behling, P. Haupttmann.Gravimetric and non-gravimetric chemical quartz crystal resonators, Seventh Technical Digest of the International Meeting for Chemical Sensors, Beijing, China, July 27–30, 1998, 121–123.
[26] E.J. Calvo, C. Danilowicz, R. Etchenique, Measurement of viscoelastic changes at electrodes modified with redox hydrogels with a quartz crystal device, J. Chem. Soc., Faraday Trans. 91 (1995) 4083–4091.
[27] F. Josse, Y. Lee, S.J. Martin, R.W. Cernosek, Analysis of the radial dependence of mass sensitivity for modified-electrode quartz crystal resonators, Anal. Chem. 70 (1998) 237–247.
[28] Q. Xie, J. Wang, A. Zhou, Y. Zhang, H. Liu, Z. Xu, Y. Yuan, M. Deng, S. Yao, A study of depletion layer effects on equivalent circuit parameters using an electrochemical quartz crystal impedance system, Anal. Chem. 71 (1999) 4649–4656.
[29] S.J. Martin, V.E. Granstaff, G.C. Frye, Characterization of a quartz crystal microbalance with simultaneous mass and liquid loading, Anal. Chem. 63 (1991) 2272–2281.
[30] R.W. Cernosek, S.J. Martin, A.R. Hillman, H.L. Bandey, Comparison of lumped-element and transmission-line models for thickness-shear-mode quartz resonator sensors, IEEE Trans. Ultrason. Ferroelectr. Freq. Control 45 (1998) 1399–1407.
[31] R. Patel, R. Zhou, K. Zinszer, F. Josse, R. Cernosek, Real-time detection of organic compounds in liquid environments using polymer-coated thickness shear mode quartz resonators, Anal. Chem. 72 (2000) 4888–4898.
[32] X. Su, C. Dai, J. Zhang, S. O'Shea, Quartz tuning fork biosensor, Biosensors Bioelectron. 17 (2002) 111–117.
[33] S.J. Xia, G. Liu, V.I. Birss, Properties of thin polystyrene films prepared on gold electrodes by the dip-coating method, Langmuir 16 (2000) 1379–1387.
[34] R.C. Weast, CRC Handbook of Chemistry and Physics, CRC Press, Boca Raton, FL, 1982.